Construction and Building Materials 449 (2024) 138549

Contents lists available at ScienceDirect

Construction and Building Materials

journal homepage: www.elsevier.com/locate/conbuildmat

Rheological and mechanical evaluation of a novel fast curing cold asphalt concrete made with asphalt emulsion, by-products and magnetic induction

Christopher DeLaFuente-Navarro [a,b], Pedro Lastra-González [a], Irune Indacoechea-Vega [a], Daniel Castro-Fresno [a,*]

[a] GITECO Research Group, Universidad de Cantabria, Avda. de Los Castros s/n., Santander 39005, Spain
[b] School of Civil Construction, Faculty of Engineering, Pontificia Universidad Católica de Chile, Avenida Vicuña Mackenna, Santiago 4860, Chile

ARTICLE INFO

Keywords:
Cold asphalt concrete
Magnetic induction
Curing process
Magnetic by-product

ABSTRACT

This work studies the feasibility of a new cold asphalt concrete with 5 % voids with fast curing, developed with asphalt emulsion and magnetic induction. Until now, it was impossible to produce fast curing cold asphalt concretes due to the impossibility of compacting and evaporating the water in the asphalt emulsion quickly. Therefore, the aim of this work is to solve the impossibility of compacting the cold asphalt concrete and thus reduce the long curing times. For this purpose, at laboratory level, an experimental cold asphalt concrete was designed with magnetic induction and compared with two reference hot asphalt concretes manufactured according to Spanish standards without magnetic induction (one with 50–70 grade bitumen and another with a PMB45/80–65 type polymer-modified bitumen). The research was carried out in two stages. First, the new cold asphalt concrete was rheologically characterized, the binder recovered from the asphalt concrete was analyzed according to the tests of ring and ball, penetration, dynamic shear rheometer (DSR) and multiple stress creep and recovery (MSCR). Secondly, the new cold concrete asphalt was mechanically characterized, the mechanical performance of the cold asphalt concrete was analyzed by evaluating stability and deformation, dry and wet indirect tensile strengths (ITS), wheel tracking test, stiffness modulus and resistance to raveling dry and wet conditions. Based on the rheological analysis results, the asphalt emulsion recovered from the cold asphalt concrete is extremely soft with a low softening point and a high penetration rate. On the other hand, the values of viscosity, phase angle, stiffness and non-recoverable creep compliance are between those of the bitumen 50/70 and the PMB45/80–65, but closer to bitumen 50/70. As for their mechanical performance, the novel cold asphalt concrete studied presents better resistance to water damage and particle loss, both in dry and wet conditions, but also high permanent deformations and low ITS, probably due to the fact that the residual binder of the emulsion used is softer than the others.

1. Introduction

The design of low-carbon asphalt mixtures has become a priority for road engineering [1]. In this regard, cold asphalt mixtures should be preferred because they are manufactured at ambient temperatures [2,3], consuming as a result less energy and generating less greenhouse gas emissions [4]. Unfortunately, it has not been possible to produce dense cold asphalt concrete with fast curing until now. This is explained by the fact that cold asphalt mixtures tend to have a high percentage of voids because of compaction difficulties due to the presence of water in the asphalt emulsion [5]. They also require a long curing time to evaporate the water contained in the asphalt emulsion [6], delaying the opening of the road.

Asphalt concrete for road surfaces should have a void content between 4 % and 6 %. Authors have tried to design more closed cold mixtures with the aim of improving their mechanical behavior [7,8], however, they only achieved a void content between 8 % and 14 % in cold asphalt mixtures [9]. So far, it is known that increasing the number of strokes by the Marshall compaction method allows a marginal decrease in air voids content [7], so researchers have opted for doubling the compaction energy on gyratory compactor [10], which is inefficient, so it is necessary to develop new manufacturing options [11].

* Corresponding author.
E-mail addresses: Christopher.delafuente@unican.es (C. DeLaFuente-Navarro), Pedro.lastragonzalez@unican.es (P. Lastra-González), Irune.indacoechea@unican.es (I. Indacoechea-Vega), castrod@unican.es (D. Castro-Fresno).

https://doi.org/10.1016/j.conbuildmat.2024.138549
Received 17 June 2024; Received in revised form 27 September 2024; Accepted 28 September 2024
Available online 2 October 2024

At the same time, the curing process of cold mixtures can take up to 28 days [12–15] depending on climate and humidity [16–18]. This is relevant because the curing process influences the performance of the cold mixture [7,19], which has a weak mechanical performance in the early stages of curing [14,20,21] and its voids content increases when the curing process ends [22].

There is currently no standardised manufacturing method for cold mixtures [23,24]. Most of the procedures developed are based on the U. S. Asphalt Institute method [7,15], which considers an initial compaction, then a curing period of 48 h at 60°C and, at the end, before the mixtures cool down, a piston compaction with a load of 178 kN for one minute, and finally cooling and demoulding. This method takes into account a long curing time and does not consider porosity parameters. Several researchers have tried to develop a new cold asphalt concrete, which improves on these shortcomings, but have been unsuccessful:

- A cold asphalt concrete with 8–9 % voids was obtained in [6]. In this work, a higher-level compaction which was called "extra-heavy compaction" was performed. Unfortunately, the designed mixture required a long curing period of 18–21 days at a constant temperature of 40°C.
- In [8], a cold asphalt concrete with palm oil fuel ash was developed. In this case, the samples were tamped ten times on the perimeter and fifteen times in the centre and then subjected to 75 blows per face. Finally, the curing also took a long time: 24 h at 40°C and then, the samples were extruded and cured for an additional 72 h period at the same 40°C.
- An asphalt concrete with emulsion and 4 % voids was achieved [22] but for this, the aggregates were heated to 120°C, which means an increase in energy consumption. Then, the samples required several compaction processes and a long curing period, since they were initially compacted by 50 blows per face and cured for 24 h at 110°C, following by a second compaction effort of 25 blows per face, ending with a further 24 h curing at room temperature.
- In [25], the influence of three Marshall compaction methods was studied (50 blows, 75 blows and double compaction). The resulting mixtures had between 8 % and 12 % voids. In addition, this research evaluated two different extensive curing processes. The first curing process cured the samples for 48 h at 60°C to leave them then for 6 h at room temperature. The second curing method cured the mixtures for 3 days at 20°C, then compacted them and finally placed them in an oven for 48 h at 60°C.
- The problem of long curing time of cold asphalt mixtures has been addressed in [26–28] with promising results using magnetic induction. However, only cold porous asphalt mixtures were evaluated.

As it can be appreciated, there is no cold asphalt concrete of dense grade with fast curing. Specifically, the mixtures that reach this level of voids require along 48 h or more of curing. In this sense, this research evaluates the feasibility of manufacturing a cold asphalt concrete by combining traditional compaction methods plus magnetic induction (a method used in other research to reduce the curing time of porous cold asphalt mixtures [28]).

In this case, magnetic induction allows the temperature of the asphalt mixture to rise quickly, evaporating the water before the compaction process independently of the weather, allowing the asphalt concrete to be compacted by traditional methods (there is not water inside the mixture) and reducing the curing time as almost all of the water contained during the manufacturing process has been already evaporated.

The particular objective of this research is to design a useful cold asphalt concrete with a commercial asphalt emulsion. For this, it is necessary to achieve an adequate curing method, a void content between 4 % and 6 % and acceptable mechanical performance. To achieve the objective of this research, a novel manufacturing protocol for an experimental cold asphalt concrete with industrial by-products was designed using magnetic induction. Thus, this research evaluates the feasibility of the novel experimental mixture with respect to two traditional reference hot asphalt concretes manufactured with two bituminous binders widely used in Europe.

The research has been structured in two main stages. In the first stage, due to the different thermal processes involved in the traditional manufacturing method in comparison with the experimental method, and the viscoelastic nature of the asphalt binders [29], the binder of the three asphalt concretes under study were recovered for rheological evaluation in terms of their softening point through the ring and ball test, their hardness with the needle penetration test, the delayed elastic response and plastic deformation with the Multi Stress Creep Recovery (MSCR) test and their viscosity, stiffness, phase angle with the dynamic shear rheometer (DSR). In addition, the master curve was determined with the results obtained in DSR. In the second stage, physical properties and the mechanical performance of the three asphalt concrete mixtures were characterized (two manufactured under European standards without magnetic induction and one experimental manufactured with magnetic induction), involving: density, voids content, stability and deformation, water sensitivity, plastic deformation, stiffness, and resistance to raveling.

2. Materials and manufacturing procedures

2.1. Materials

Three different types of binders have been used for this investigation: a 50–70 penetration grade bitumen, a PMB 45/80–65 polymer modified bitumen and a C60BP4-MIC polymer modified emulsion. The properties of the three binders are summarised in Table 1.

The aggregates used were ophite for the coarse fraction and limestone for the fine and filler fractions. Their main properties are summarised in Table 2. In addition, a magnetic industrial by-product called "steel shot blasting" (Fig. 1) was used to improve the electrical properties of the experimental cold asphalt concrete [30]. This industrial by-product was already used in a previous research [31]. Due to its size and spherical shape, it does not require a previous preparation process, it is uniformly distributed in the mixture and does not generate steel clusters. Their density and the percentage of particles passing through each sieve size are summarized in Table 3.

2.2. Manufacturing procedures

For the development of this research, Marshall type samples were fabricated. Three types of asphalt concrete with AC16 particle size distributions according to EN 933–1 were developed: a reference mixture

Table 1
Binder properties.

Binder type	Test	Value	Standard
Bitumen grade 50/70	Penetration (25°C, mm/10)	57	EN 1426
	Specific Gravity	1.04	EN 15326
	Softening point (°C)	51.6	EN 1427
	Ductility force (5°C, J/cm2)	-	-
	Elastic recovery (25°C, %)	-	-
Bitumen PMB 45/80–65	Penetration (25°C, mm/10)	56.00	EN 1426
	Specific Gravity	1.03	EN 15326
	Softening point (°C)	74.10	EN 1427
	Ductility force (5°C, J/cm2)	3.11	EN 13589
	Elastic recovery (25°C, %)	88.00	EN 13398
Emulsion C60BP4-MIC	Polarity	Positive	-
	Breakage value (g)	180	EN 13075–1
	Residual binder content (%)	61	EN 1428
	Creep time (2 mm, 40°C)	45	EN 12846–1
	Settling tendency (7 days)	7.5	EN 12847
	Sifting residue (0.5 mm)	0.03	EN 1429
	Penetration (mm/10, 25°C)	100	EN 1426
	Softening point (°C)	50	EN 1427

Table 2
Aggregates properties.

Aggregate type	Property	Value	Limit	Standard
Ophite	Los Angeles coefficient	13	≤ 20	EN 1097–2
	Specific weight (g/cm3)	2.787	-	EN 1097–6
	Polished stone value (PSV)	60	≥ 56	EN 1097–8
	Flakiness Index (%)	8	≤ 20	EN 933–3
Limestone	Los Angeles coefficient	28	-	EN 1097–2
	Specific weight (g/cm3)	2.705	-	EN 1097–6
	Sand equivalent	78	> 55	EN 933–8
Hydrated lime	Specific weight (g/cm3)	1.959	-	EN 1097–6

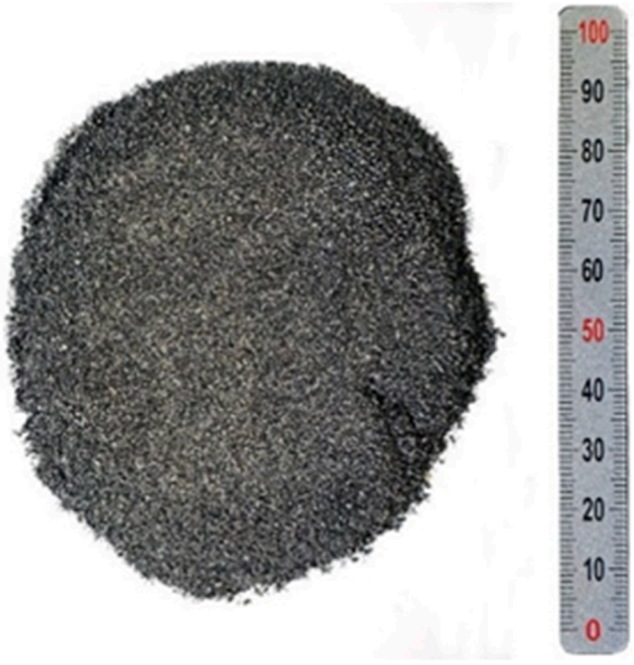

Fig. 1. Magnetic by-product: Steel shot blasting.

with conventional 50/70 penetration grade bitumen (AC 50–70); a second reference mixture with a PMB 45/80–65 bitumen (AC PMB) and, thirdly, the experimental cold mixture with asphalt emulsion type C60BP40-MIC (Cold AC). Magnetic aggregate was only added to the experimental mixture, dosed at 5 % by volume to ensure its homogeneous distribution in the mixture and to avoid the formation of clusters [32–34]. The particle size distribution of the three asphalt concretes is shown in Fig. 2.

The manufacture of the two reference asphalt concretes (AC 50-70 and AC PMB) was in accordance with the Spanish standard (EN 12697-30), so magnetic induction was not used in their manufacture. Thus, the procedure being as follows: the coarse and fine fraction are firstly mixed, then the bitumen and finally the filler fraction are added. Regarding the manufacturing temperature, the aggregates are heated for 6 h to reach the temperature based on the bitumen specifications (150°C for the AC 50-70 mixture and 165°C for the AC PMB).

With regard to the experimental mixture, the impossibility of compressing the water contained in the asphalt emulsion makes the manufacture of Cold AC difficult. For this reason, a novel procedure for manufacturing the experimental mixture using magnetic induction was designed.

In the proposed method, the coarse and fine fraction are mixed with the asphalt emulsion for two minutes, then the magnetic aggregate and filler fraction are added and mixed with the rest for two minutes, all at room temperature. Once all materials have been mixed, the mixture is exposed to a magnetic field according to the protocol in Table 4, designed as developed in [28], with the aim of evaporating the water contained in the emulsion by rapidly reaching the boiling temperature of water. Once the magnetic induction protocol was completed, the mixture was compacted by 75 strokes on each side using the Marshall compactor. Finally, Cold asphalt concrete with 5 % voids manufactured by magnetic induction has hardened and achieved room temperature after 50 min from the end of its manufacture. This time was obtained by measuring the temperature and total weight of the compacted mixture every 2 min. It should be noted that this is a significant reduction in curing time compared to that reported by other authors to date [6,8,22,25].

The intensities were designed from the magnetic particles, since their shape, size, homogeneity and purity affect their sensitivity to magnetic fields [35–38]. The magnetic field was applied by means of a high-frequency magnetic induction equipment (EasyHeat LI 3542). The coil was placed at a fixed distance of 1 cm from the sample surface. It should be noted that this parameter has a significant influence on the effectiveness of magnetic induction heating [39–42].

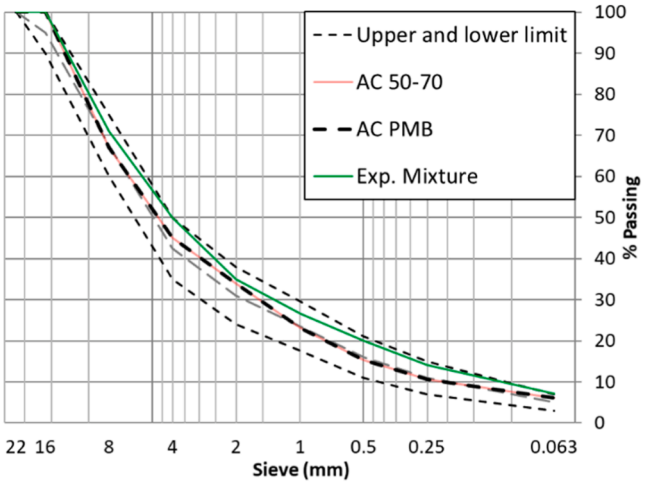

Fig. 2. Granulometric distribution.

Table 4
Magnetic induction protocol.

	Step	Intensity (A)	Power (W)	Time (minutes)	Frequency (KHz)
Experimental protocol	1	300	1560	3	185
	2	160	550	2	185
	3	130	20	30	185

Table 3
Magnetic by-product properties: density and percentage passing through each sieve size.

Magnetic by-product	Density	Sieve (mm)						
	(g/cm3)	8	4	2	1	0.5	0.25	0.063
Steel shot blasting	7.435	100 %	100 %	100 %	100 %	67 %	14 %	0 %

3. Research methodology

A rheological analysis was performed on the residual binder, because the manufacturing method used in the experimental mixture is new and the rheological consequences of the application of magnetic induction are not known. In addition, a mechanical evaluation of the experimental asphalt concrete was performed to ensure adequate performance, as until now, no cold asphalt concrete has been produced that meets the requirement for air voids content with rapid curing.

3.1. Rheological evaluation

After the manufacturing process of the three mixtures under study, the binder was recovered by the rotary evaporator method (EN 12697-3). The recovered binder samples were characterised including empirical and rheological properties (i.e. softening point, penetration, shear recovery, viscosity, stiffness, phase angle and, finally, the master curve was also determined).

3.1.1. Ring and ball and penetration test

Softening point and hardness of the binders were determined according to the Ring and Ball method (EN 1427:2015) and needle penetration test (EN 1426:2015), respectively. Concerning the Ring and Ball, this test starts at 5°C and the temperature is increased by 5 °C/min until two steel balls of 9.5 mm diameter and 3.5 g, wrapped on bitumen, reach a depth of 25±0.4 mm. As for the needle penetration test, the temperature is set at 25°C and a 100 g needle is dropped in free fall on the binder and the penetration achieved after 5 s is measured in tenths of a millimeter (dmm). This process is repeated six times.

3.1.2. Dynamic shear rheometer (DSR)

Viscosity, stiffness and phase angle were determined using the Dynamic shear rheometer (DSR) test according to EN 14770:2024. This test is performed from 60°C to 10°C at 5°C intervals and the frequencies tested ranged from 0.1 Hz to 30 Hz. Then, because frequency and temperature directly affect the performance of the asphalt binder, the results were normalised by developing the master curve according to the method employed in [43,44]. Thus, the complex shear modulus data is fit to a sigmoidal function by least-squares:

$$\log(|G^*|) = \eta + \frac{\beta}{1 + e^{\gamma - \mu \log(f_r)}} \quad (MPa) \tag{1}$$

Where γ and μ are shape parameters, η is the lower asymptote, β is the variance between the asymptotes' values and f_r is the reduced frequency, as defined by Eq. 2.

$$f_r = A_t \bullet f \left(\frac{rad}{s}\right) \tag{2}$$

Where the Time-temperature shift factor (A_t) is estimated according to Eq. 3 and f is frequency.

$$\log(A_t) = A_1 T^2 + A_2 T + A_3 \tag{3}$$

Where T is the temperature (°C) and A_1, $A_2 and A_3$ are fitting parameters.

3.1.3. Multiple stress creep recovery (MSCR test)

Shear creep recovery was determined by the MSCR test (EN16659:2016). In this test, two parameters are determined: the elastic recovery (%R) and the non-recoverable creep compliance (J_{nr}), being the latter representative of the material's susceptibility to plastic deformation [45–47]. As specified in the standard, 25 mm diameter circular binder samples are used and the test is carried out at 60°C applying 10 loading cycles at two different stress levels of 0.1kPa and 3.2 kPa. Each cycle took 10 s, 1 s for loading and 9 s for recovery. The average values of %R and Jnr at creep stress levels of 0.1 kPa and 3.2 kPa are calculated as the average of the values obtained in each cycle according to Eqs. 4 to 9.

$$\%R^N_{0.1kPa} = \frac{100 \bullet (\varepsilon^N_1 - \varepsilon^N_{10})}{\varepsilon^N_1} \tag{4}$$

$$\%R^N_{3.2kPa} = \frac{100 \bullet (\varepsilon^N_1 - \varepsilon^N_{10})}{\varepsilon^N_1} \tag{5}$$

$$J^N_{nr0.1kPa} = \frac{\varepsilon^N_{10}}{0.100} \tag{6}$$

$$J^N_{nr3.2kPa} = \frac{\varepsilon^N_{10}}{3.200} \tag{7}$$

$$\varepsilon^N_1 = \varepsilon^N_c - \varepsilon^N_0 \tag{8}$$

$$\varepsilon^N_{10} = \varepsilon^N_r - \varepsilon^N_0 \tag{9}$$

Where ε^N_1 is the deformation at the end of the creep part of each cycle. ε^N_{10} is the final strain of the creep part. ε^N_0 is the absolute deflection at the beginning of cycle N. ε^N_c is the absolute value of the deflection at the end of the creep part of each cycle. ε^N_r is the absolute value of the deformation at the end of the deformation part of each cycle.

3.2. Mechanical evaluation

After the manufacturing process, the reference and experimental asphalt concretes were characterised and mechanically tested, according to Spanish standard to assess their feasibility. In this sense, density, total voids, stability and deformation, indirect dry and wet tensile strengths, deformation and rutting slope were determined. In addition, to gain a better understanding of the new asphalt concrete, the stiffness modulus and the dry and wet particle loss were evaluated. It should be noted that eight Marshall samples were tested for each test. With the exception of the deformation slope and rutting depth, two lanes of each type of asphalt concrete were tested.

3.2.1. Density, total voids, stability and deformation

The density was determined according to EN 12697-5 while total voids respect to EN 12697-8. For voids, Eq. 10 was used, where m_{dry} is the mass of the sample in dry condition, V is the geometric volume of the sample and G_{mm} is the theoretical specific weight of the mixture.

$$Total\ air\ voids(\%) = \left(1 - \frac{m_{dry}}{V \bullet G_{mm}}\right) \times 100 \tag{10}$$

Stability and deformation were determined by the Marshall test according to EN 12697-34. The test was performed at room temperature, the loading rate was 50 mm/min.

3.2.2. Indirect tensile strength (ITS)

The indirect tensile strength in kPa in dry and wet conditions was calculated using the water sensitivity test according to EN 12697-12. The test was carried out at 15°C and the loading rate was 50 mm/min. The wet samples were placed in a water bath at 40°C for 72 h. Finally, the ITSR (%) was calculated to evaluate the sensitivity of each mixture to the effect of water.

3.2.3. Deformation slope and rutting depth

The deformation slope and rut depth were determined with the wheel tracking test according to EN 12697-22. The test specimens were conditioned at the test temperature for 4 h. The test was run at 60°C, 20,000 cycles were applied with a pneumatic wheel and a load of 700 N was applied.

3.2.4. Stiffness modulus

The stiffness modulus it was determined according to EN 12697-26. The specimens were air-conditioned for 24 h. The test was carried out at 20°C and stress pulses were applied until a horizontal deformation of 0.005 % of the specimen diameter was reached. The modulus of rigidity was calculated using Eq. 11.

$$E(Mpa) = \frac{F \bullet (v + 0.27)}{(z \bullet h)} \quad (11)$$

Where E is the modulus of rigidity in Mpa, F is the maximum load, z the horizontal deformation, h the specimen thickness and v the Poisson coefficient.

3.2.5. Particle loss

Raveling is not a common failure in asphalt concrete mixtures. However, as Cold AC mixture is completely new and there are no previous records of its possible mechanical performance, the cohesion of the experimental mixtures was assessed using the Cantabro test (EN 12697-17), both at dry and wet conditions. The samples were air-conditioned for 24 h and the test was carried out at 25°C at a speed of 33 revolutions per minute. The particle loss was determined by Eq. 12.

$$M_L(\%) = \frac{m_i - m_f}{m_i} \times 100 \quad (12)$$

Where, M_L is the mass loss in percentage. m_i is the initial mass and m_f is the final mass.

4. Results and discussion

4.1. Rheological evaluation

4.1.1. Ring and ball and penetration test

Table 5 summarises the results of the ring and ball and penetration tests. The binder recovered from AC PMB has a higher softening point and a lower penetration rate than the binders in Cold AC and AC 50–70, being the results statistically significant in both cases (Table 6). In addition, the binder recovered from Cold AC is the softest of the three, which may lead to plastic deformation problems in the performance of cold asphalt concrete.

4.1.2. Dynamic shear rheometer (DSR)

Fig. 3 summarises the results of the viscosity measured with the DSR. Although the viscosity of the materials is very similar at low temperatures, as the temperature increases, the polymer modified binders seem to require higher temperatures to decrease their viscosity. Furthermore, at high frequencies, the viscosity differences between the three binders are reduced. Specifically, the binder recovered from AC 50–70 is the binder with the lowest resistance to displacement at all frequencies and temperatures. For this reason, AC 50–70 is expected to have a better aggregate envelopment at the time of manufacture, since binders with lower viscosity mix more easily with the aggregates [48]. This result is significant with respect to the binder recovered from AC PMB (Table 7). In addition, Cold AC has an intermediate viscosity value and despite being modified with polymers, behaves much more like the binder recovered from AC 50–70. However, in this case, the result does not present statistically significant differences with respect to the rest of viscosities.

Table 5
Softening point and penetration test results.

Mixture	Softening point (°C)		Penetration (dmm)	
	Initial state	recovered after manufacturing	Initial state	recovered after manufacturing
AC 50–70	51.6	54.6 ± 0.3	57.0	53.2 ± 1.3
AC PMB	74.1	72.3 ± 1.7	56.0	40.1 ± 1.5
Cold AC	50.0	50.5 ± 0.6	100.0	64.9 ± 1.2

Table 6
p-values ring and ball and penetration test.

Mixture	p- value			
	Ring and ball	Status	Penetration	Status
AC 50–70 - AC PMB	0.025	Significant	0.019	Significant
AC 50–70 - Cold AC	0.042	Significant	0.027	Significant
AC PMB - Cold AC	0.031	Significant	0.014	Significant

Fig. 4 shows the stiffness results for each of the binders measured with the DSR. The AC PMB binder is significantly stiffer than those of AC 50–70 and Cold AC (Table 8), so it is probable that it performs better under plastic deformation. At the same time, the stiffness values of the AC 50–70 and Cold AC binders had no statistically significant differences despite the fact that the Cold AC binder is polymer modified. Importantly, as the temperature increases, a decrease in the stiffness of the three asphalt binders is observed, this is because the viscous component increases in all three binders irrespective of the test frequency. Note that, with increasing temperature, the stiffness values of the three binders start to become increasingly different, which can be attributed to the fact that the AC 50–70 binder has no polymers in its composition to help it maintain its stiffness once the binder has softened.

Fig. 5 shows the phase angle results measured with the DSR. In all cases, as the temperature increases, the phase angle increases. Specifically, The binder of AC 50–70 presents the highest phase angle, irrespective of temperature and frequency, and this result is statistically significant when compared to that of AC PMB but not with Cold AC phase angle (Table 9). Specifically, the phase angle of the AC 50–70 binder at low frequencies increases with temperature to almost reach a maximum of 90°, so it would behave as a purely Newtonian fluid in this range. This indicates that the binder of AC 50–70 binder has a lower elasticity and a higher deformation capacity than the rest of the binders, which can be explained by the fact that it is the only binder from those studied in this work that is not modified with polymers. Furthermore, the PMB type ligand has a fairly homogeneous behavior with respect to its phase angle at different temperatures and frequencies, a result that coincides with that shown by Lagos-Varas in [49].

Fig. 6 shows the master curves of the binders recovered from the three asphalt concrete mixtures. The master curve shows the susceptibility to temperature and loading frequency variables. In this respect, the AC PMB binder has the highest complex modulus, irrespective of temperature and frequency. However, as the frequency increases, the performance of the different binders becomes more and more similar. In addition, the master curves of AC 50-70 and Cold AC show a very similar behaviour at all times. This result agrees with the study of viscosity, stiffness and phase angle, where no significant differences were obtained between the results of the two binders.

4.1.3. Multiple stress creep recovery test

Fig. 7 shows the MCSR test results at 0.1 kPa and 3.2 kPa. Cold AC binder exhibited the largest deformations, this makes sense considering that the penetration and ring and ball results revealed it as the softest binder of the three studied. At the same time, AC PMB showed the lowest deformation values. For this reason, the binder of AC PMB binder is likely less susceptible to the action of applied loads, which would also make it less prone to micro-cracking.

The AC PMB binder had the highest recovery rates (Table 10) and the difference compared to the other two binders is statistically significant (Table 11). The Cold AC binder had the second highest recovery rate and although the difference with that of AC 50–70 binder is low, it is statistically significant. In other words, the Cold AC showed an elastic behavior after the experimental cure method.

Lower Jnr values suggest better rutting performance because the

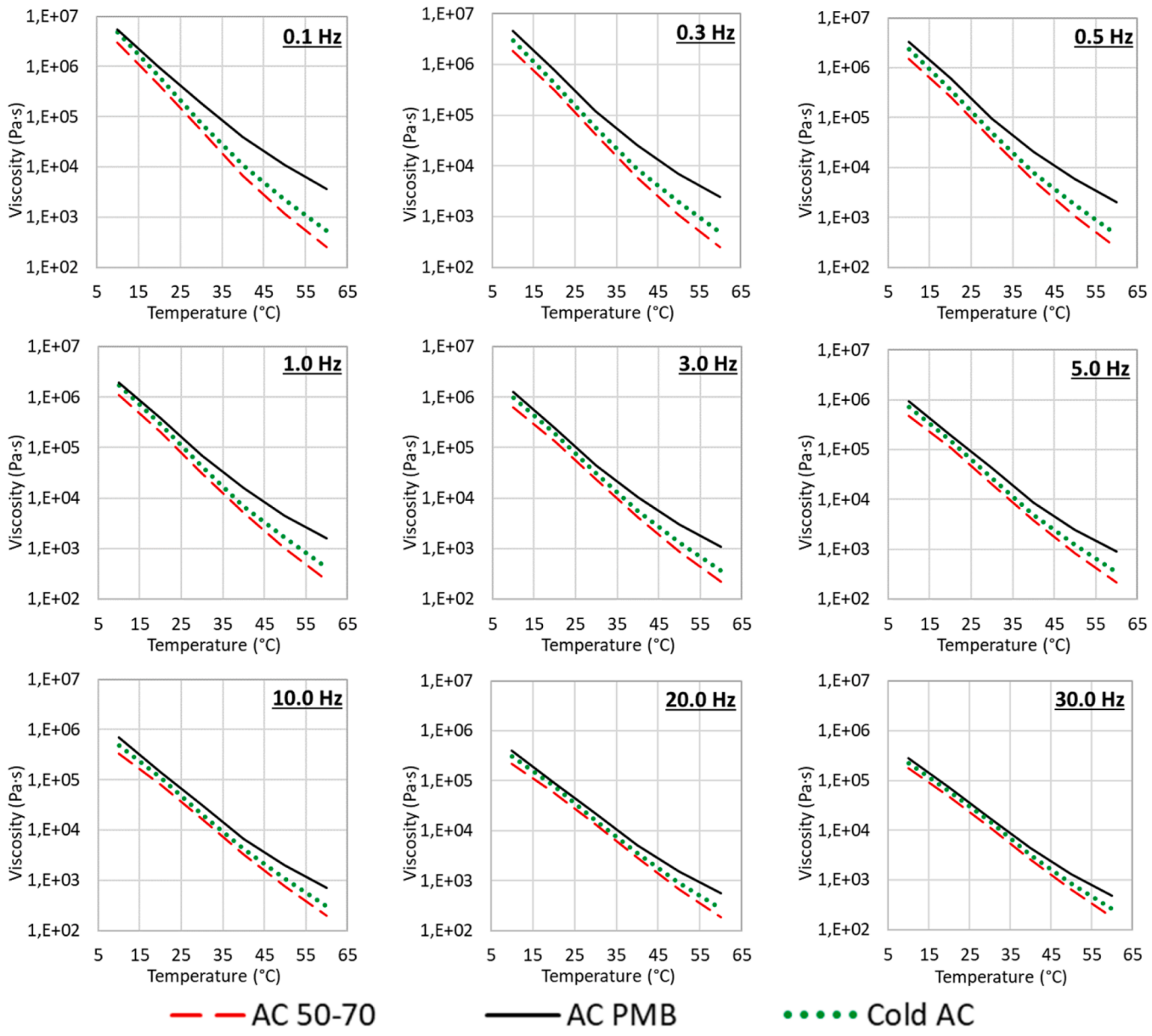

Fig. 3. Dynamic shear rheometer results: viscosity.

Table 7
P-values DSR test results: viscosity.

Residual binder	p- value	
	Viscosity	Status
AC 50–70 - AC PMB	0.017	Significant
AC 50–70 - Cold AC	0.228	Not significant
AC PMB - Cold AC	0.096	Not significant

bitumen is less susceptible to permanent stress accumulation and therefore, there is a higher binder contribution to the resistance of the asphalt concrete to permanent deformation [50]. In this respect, the binder of AC PMB has the lowest creep values (Table 10), being the difference with the other results statistically significant (Table 12), suggesting that it will have the best rutting performance. The binder of Cold AC does not present statistically significant differences with respect to AC 50–70.

Fig. 8 shows the plot of recovery (%R) versus creep (jnr) together with the modification curve, which is an indicator of elasticity according to AASHTO M 332–23. For this, the results of the 3.2 kPa load test are considered, as they correlate better with the permanent deformation behaviour of asphalt mixtures [51]. In this sense, only the AC PMB binder exhibits high elasticity with good elastomeric behaviour [52]. On the other hand, both the Cold AC binder and the reference mixture are below 0.5 kPa-1 (Fig. 8), so they can be applied on roads with extreme traffic [53].

4.2. Mechanical evaluation

4.2.1. Density, total voids, stability y deformations

The application of magnetic induction allows cold asphalt concrete with industrial by-products to be manufactured with the same percentage of voids as the reference asphalt mixtures, even reducing variability (Table 13). Therefore, the magnetic induction fabrication method developed in this research significantly reduces the percentage of voids achieved in previous studies [6,8,22,25]. The voids content is practically the same in the three asphalt concrete mixtures, so it is ruled out that the internal structure of the mixtures is a factor to be considered in the

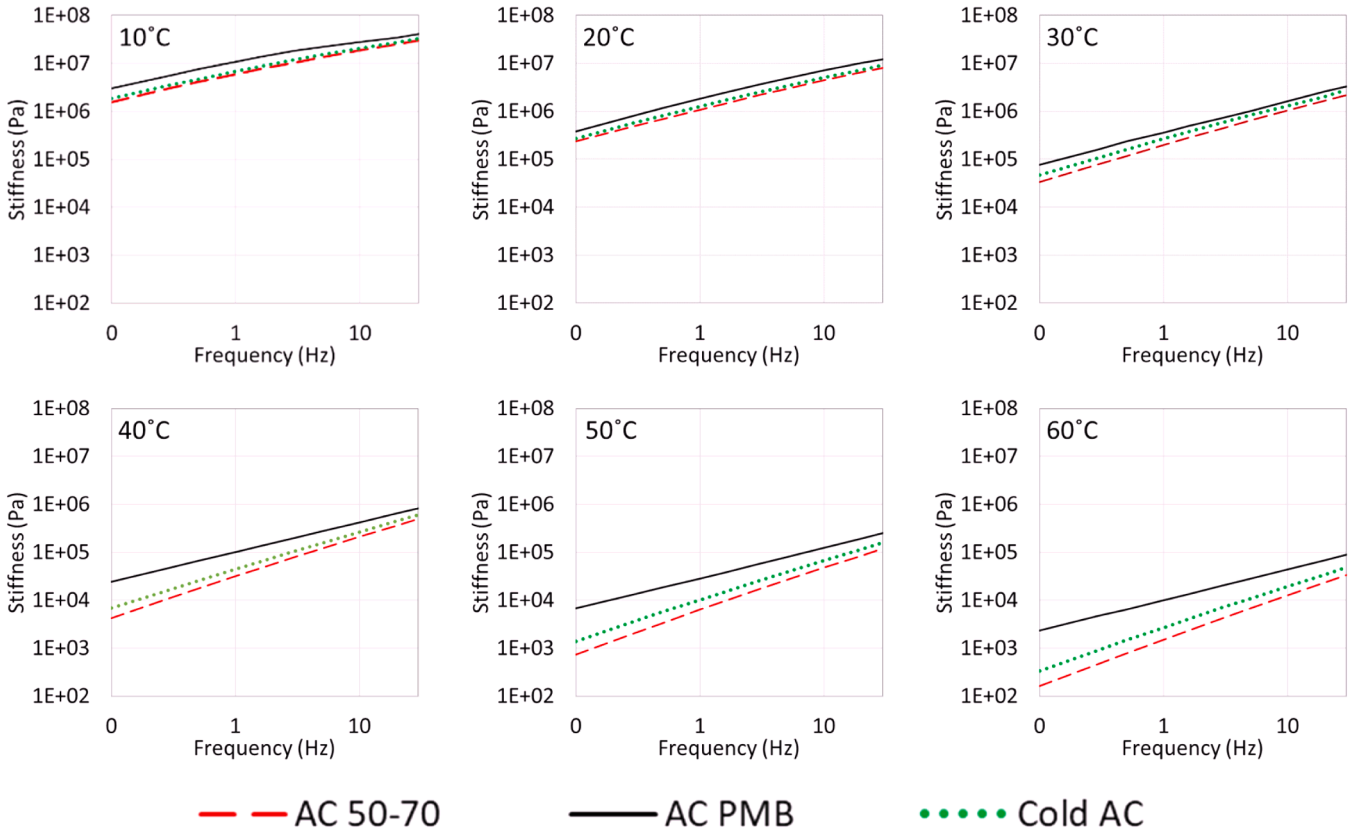

Fig. 4. DSR test results: stiffness.

Table 8
P-values DSR test results: stiffness.

Residual binder	p- value	
	Stiffness	Status
AC 50–70 - AC PMB	0.031	Significant
AC 50–70 - Cold AC	0.339	Not significant
AC PMB - Cold AC	0.025	Significant

mechanical evaluation.

Considering the above, the deformation and stability results show the high influence of the type of binder used on the mechanical performance of asphalt concrete (Table 13). Initially, AC 50–70 presents the lowest degree of deformation. Then, AC PMB is shown as the mixture with the highest stability. Finally, Cold AC is the one with the lowest stability with higher deformations than those shown by the reference mixtures, being this result statistically significant (Table 14). This can be explained by the rheological study, the binder of Cold AC is the softest (i.e higher penetration rate).

Table 9
P-value DSR test results: phase angle.

Residual binder	p- value	
	Phase angle	Status
AC 50–70 - AC PMB	0.000	Significant
AC 50–70 - Cold AC	0.422	Not Significant
AC PMB - Cold AC	0.000	Significant

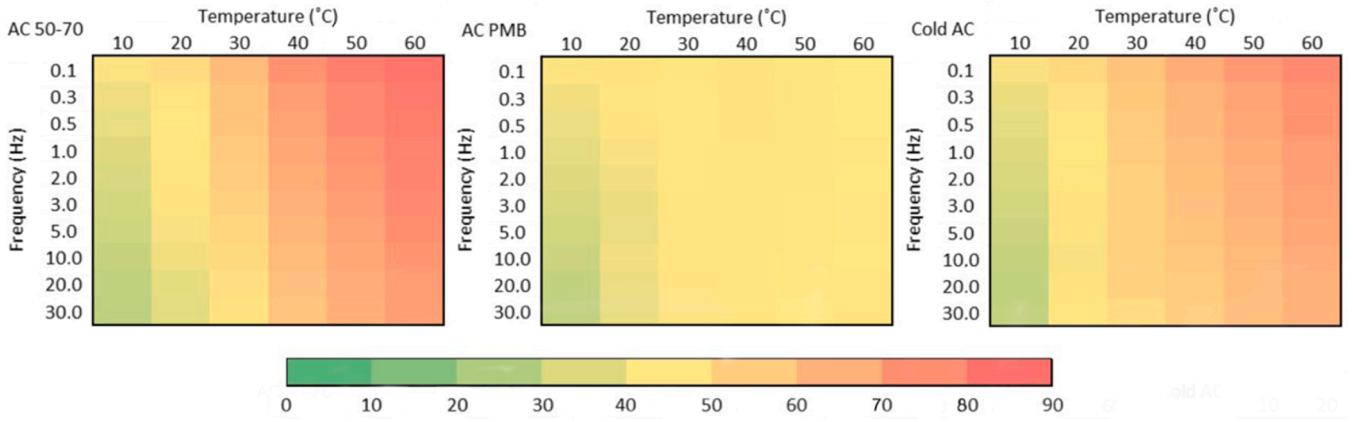

Fig. 5. Dynamic shear rheometer: phase angle.

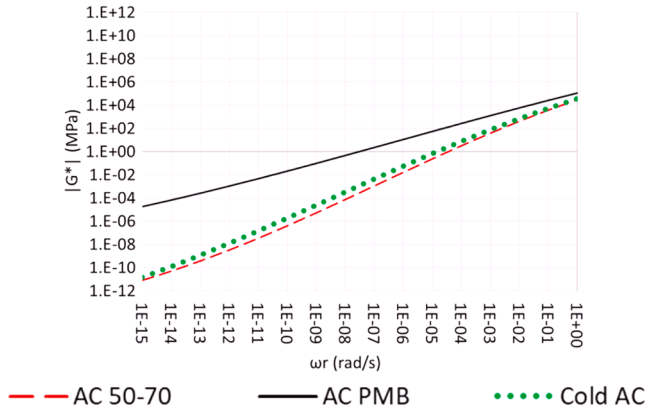

Fig. 6. Master Curve.

4.2.2. Indirect tensile strength (ITS)

The results of the indirect tensile strength test are summarised in Fig. 9. The three mixtures under study had an ITSR above 80 %, showing a fairly similar sensitivity to water. In the case of Cold AC, water damage is not a cause for concern, since it showed the lowest susceptibility to water and complies with the requirements established by the European technical specifications for road works (EN 13108-1). However, Cold AC presents significantly lower indirect tensile strengths compared to the reference mixtures (Table 15), this can be attributed to the softer binder in this mixture, which is supported by the penetration and ring and ball results. It should be noted that the addition of steel shot to Cold AC should not contribute to the indirect tensile strength due to its spherical shape, which does not contribute to the cohesion of the mixture.

The highest ITS values correspond to AC PMB, a statistically significant result (Table 15). The increase in the indirect tensile strength can be attributed to the higher stiffness of the binder in this mixture, which is supported by the results obtained in the master curves where the stiffness of the AC PMB binder was always higher than that of the other two binders.

4.2.3. Resistance against plastic deformation

Fig. 10 and Table 16 shows the results of the wheel tracking test to evaluate the performance in terms of the resistance to plastic deformation of the mixtures exposed to high temperatures. In this regard, Cold AC had the highest slope and rut depth, which were significantly different from those of the reference mixes, AC 50–70 and AC PMB (Table 17). The slope and rut depth results of Cold AC suggest that the mixture is less stable and less resistant to flow force. Although Cold AC had steel shot particles, the low level of high temperature resistance can be explained by the mechanical properties of the binder used in this experimental mix, which is very soft with a high degree of penetration and a low softening temperature. For this reason, if this method is extended, it would be necessary to use new emulsions with lower penetration grade, closer to conventional 50/70 bitumen.

Ref. PMB presents the lowest value of slope and rut depth (Fig. 10). This is explained by the binder used in this type of mixture, which is in line with the higher stiffness, lower penetration and higher softening point of this binder compared to the other two. In conclusion, Ref. PMB

Table 10
MSCR test results: recovery and Jnr.

Residual binder	0.1 kPa		3.2 Kpa	
	Recovery (%)	Jnr (kPa-1)	Recovery (%)	Jnr (kPa-1)
AC 50–70	5.016	0.242	0.910	0.283
AC PMB	76.432	0.006	75.881	0.007
Cold AC	14.942	0.137	5.400	0.165

Table 11
p-value MCSR test results: recovery.

Residual binder	p- value			
	Recovery (0.1 Kpa)	Status	Recovery (3.2 Kpa)	Status
AC 50–70 - AC PMB	0.001	Significant	0.000	Significant
AC 50–70 - Cold AC	0.00	Significant	0.001	Significant
AC PMB - Cold AC	0.001	Significant	0.000	Significant

Table 12
P-value MCSR test results: Jnr.

Residual binder	p- value			
	Jnr (0.1 Kpa)	Status	Jnr (3.2 Kpa)	Status
AC 50–70 - AC PMB	0.001	Significant	0.000	Significant
AC 50–70 - Cold AC	0.061	Not Significant	0.348	Not Significant
AC PMB - Cold AC	0.001	Significant	0.000	Significant

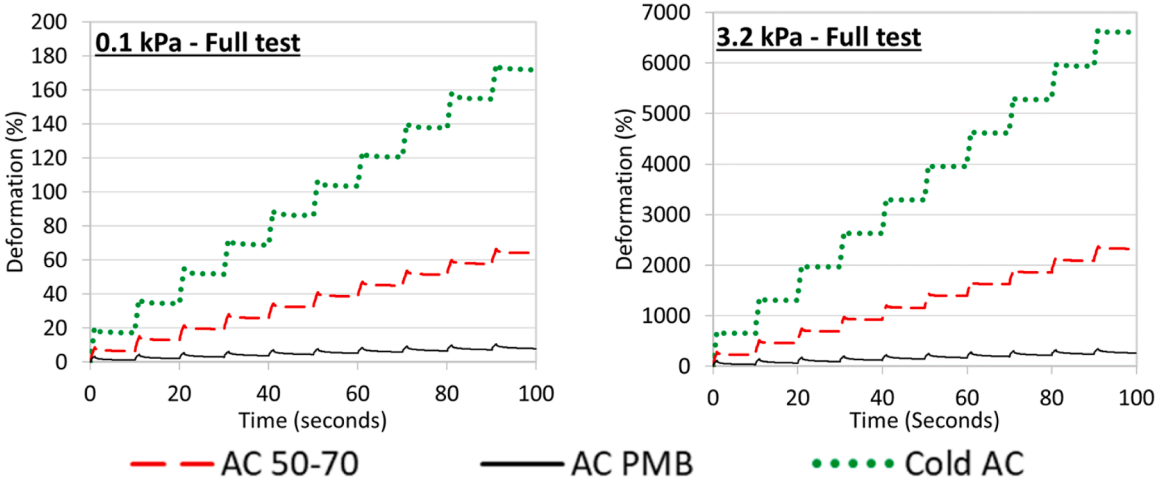

Fig. 7. MSCR test results.

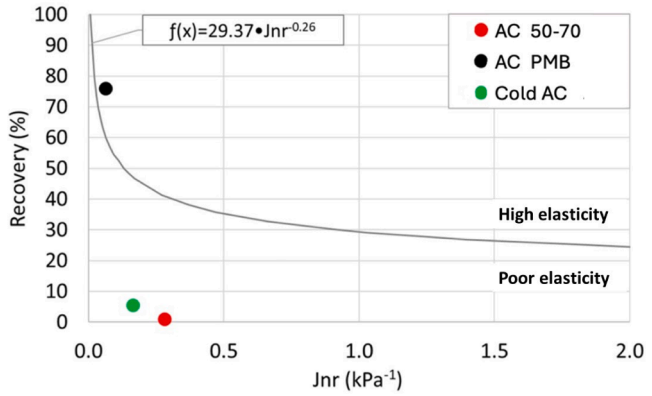

Fig. 8. Elasticity curve of recovery vs. Jnr.

Table 13
Density, total voids and results of the Marshall test.

Mixture	density (g/cm3)	voids (%)	Deformation (mm)	Stability (kp)
AC 50–70	2.538	4.8 ± 0.4	3.2 ± 0.3	1104 ± 8.0
AC PMB	2.521	4.9 ± 0.3	4.6 ± 0.7	1751 ± 86
Cold AC	2.623	4.8 ± 0.2	5.4 ± 0.8	687 ± 57

Table 14
P-values of deformation and stability test results.

Mixture	p- value			
	Deformation	Status	Stability	Status
AC 50–70 - AC PMB	0.008	Significant	0.000	Significant
AC 50–70 - Cold AC	0.013	Significant	0.002	Significant
AC PMB - Cold AC	0.227	Not significant	0.000	Significant

presents the best performance at high temperatures in terms of rutting, being this result statistically significant (Table 17).

4.2.4. Stiffness modulus

Fig. 11 shows the load applied to reach the transient horizontal deformation of 0.005 % of the specimen diameter and the results of the stiffness modulus of the three asphalt concretes. In this respect, Cold AC has the lowest stiffness modulus, and the difference with the stiffness modulus of the AC 50–70 and AC PMB mixes is statistically significant (Table 18). This result suggests that Cold AC deforms easily because it is the softest of the binders studied. In addition, the mixture has a very soft binder so it will require lower loads to deform than other mixtures containing a harder or stiffer binder, as it is the case with the reference mixtures.

4.2.5. Particle loss

Fig. 12 summarizes the particle loss results of the three asphalt concretes, both at dry and wet conditions. In this respect, the three mixtures show exceptionally good results, result consistent with the fact that they have a very low percentage of voids. Cold AC shows the best resistance to particle loss and this result is statistically significant with respect to AC 50–70 but not with respect to AC PMB (Table 19). This can be explained by the fact that the polymer-modified binders used in AC PMB and Cold AC increase the elasticity of the asphalt concretes. Furthermore, as in the ITS test, Cold AC showed the lowest susceptibility to the effect of water, a very important characteristic considering that asphalt concretes do not have the capacity to evacuate rainwater.

5. Conclusions

In conclusion, a novel cold asphalt concrete has been developed with fast curing industrial by-products by means of magnetic induction. In this respect, it is possible to conclude the following:

- The novel manufacturing method with magnetic induction solves the impossibility of manufacturing cold asphalt concrete with asphalt emulsion.
- Cold asphalt concrete with 5 % voids, manufactured by magnetic induction, has hardened and achieved room temperature after 50 min from the end of its manufacture.
- Cold AC presents a low mechanical performance at high temperatures. To address this constraint, new asphalt emulsions with residual bitumen with a penetration rate closer to 50–70 are required, as far as this method does not age significantly the residual binder.
- Cold AC residual bitumen is significantly softer than AC 50–70 and AC PMB residual binder because it has a lower softening point and a higher penetration rate. In addition, Cold AC residual binder has a viscosity, phase angle and stiffness intermediate between AC 50–70 and AC PMB residual binder. However, when evaluating the MSCRT results, the Cold AC binder presents an intermediate recovery capacity but it is the one that accumulates the highest deformation in the test because it is softer than the AC 50–70 and AC PMB binders.
- Cold AC has better particle loss performance than AC 50–70 and AC PMB. In addition, Cold AC appears to be less susceptible to water damage in the indirect tensile test. However, Cold AC has a lower

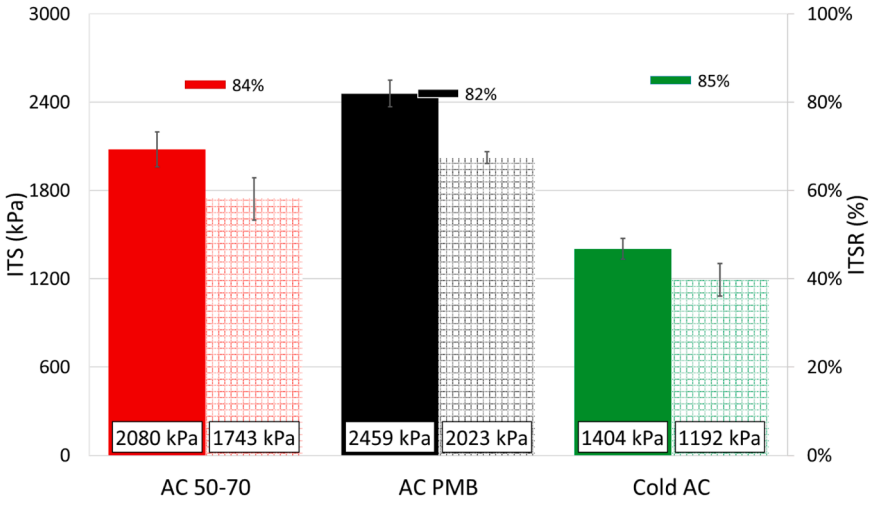

Fig. 9. Indirect tensile strength test results.

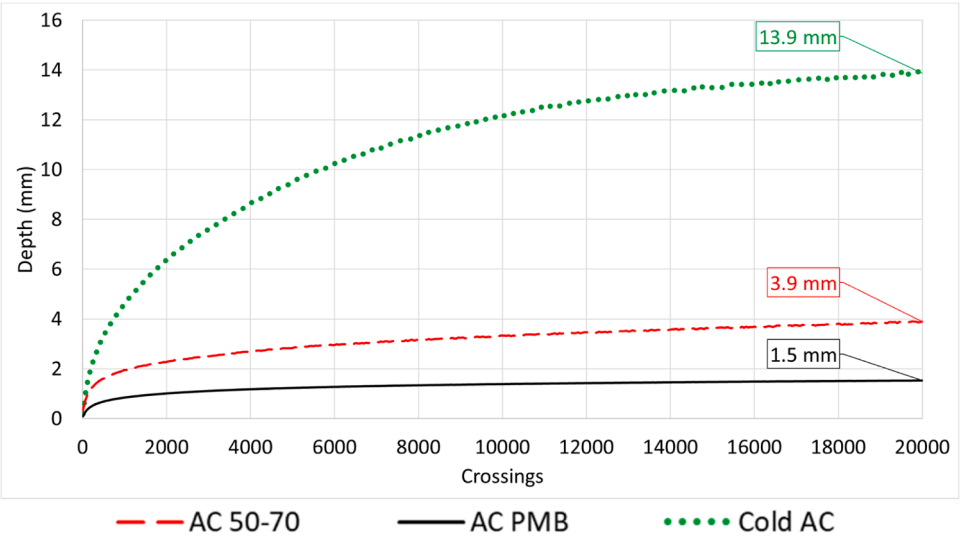

Fig. 10. wheel tracking test results: Depth.

Table 15
P-value indirect tensile strength test results.

Mixture	p- value			
	Dry condition	Status	Wet condition	Status
AC 50–70 - AC PMB	0.003	Significant	0.030	Significant
AC 50–70 - Cold AC	0.000	Significant	0.023	Significant
AC PMB - Cold AC	0.000	Significant	0.004	Significant

Table 16
Wheel tracking slope.

Mixture	Wheel-tracking slope (mm/1000 cycles)
AC 50–70	0.11 ± 0.02
AC PMB	0.03 ± 0.01
Cold AC	0.33 ± 0.05

Table 17
P-values Rutting test results.

Mixture	p- value			
	Depth	Status	Wheel-tracking slope	Status
AC 50–70 - AC PMB	0.042	Significant	0.039	Significant
AC 50–70 - Cold AC	0.000	Significant	0.007	Significant
AC PMB - Cold AC	0.000	Significant	0.000	Significant

Table 18
P-value stiffness test results.

Mixture	p- value	
	Stiffness Modulus	Status
AC 50–70 - AC PMB	0.001	Significant
AC 50–70 - Cold AC	0.000	Significant
AC PMB - Cold AC	0.004	Significant

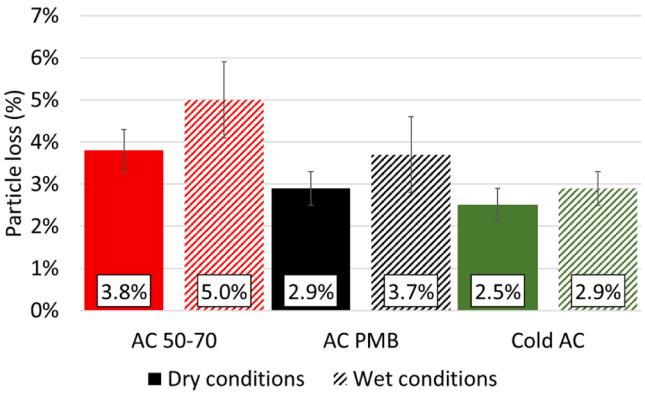

Fig. 12. Particle loss test results.

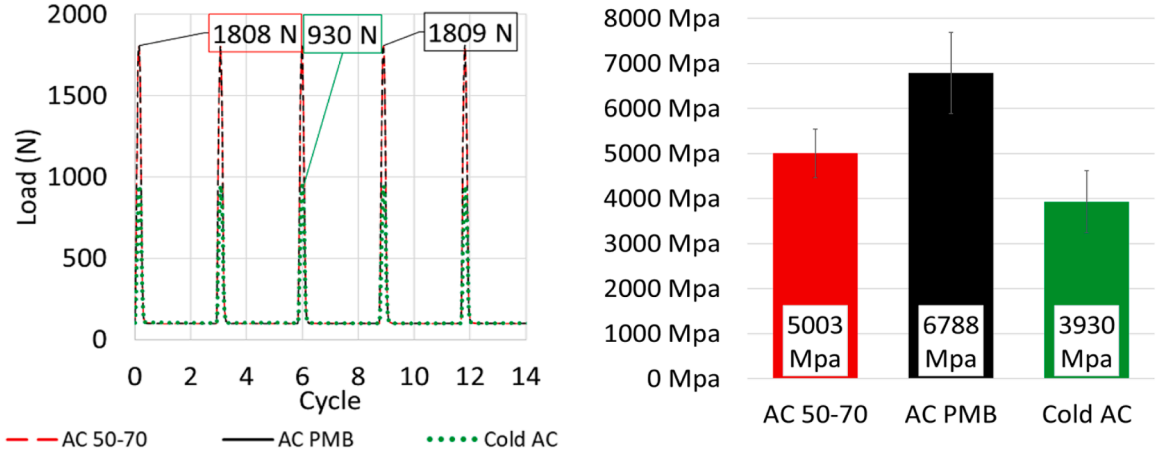

Fig. 11. Stiffness test results.

Table 19
P-value particle loss test.

Mixture	p- value			
	Dry condition	Status	wet condition	Status
AC 50–70 - AC PMB	0.014	Significant	0.051	Not significant
AC 50–70 – Cold AC	0.004	Significant	0.005	Significant
AC PMB – Cold AC	0.226	Not significant	0.101	Not significant

stiffness modulus and higher plastic deformations than the reference mixtures because its binder is softer than the others.

It is possible to manufacture new asphalt concrete using an emulsion with 5 % voids by magnetic induction. However, it is clear that the type of binder applied has a significant influence on the mechanical performance of asphalt concrete. For this reason, Future work will address the limitations and areas of improvement of this technology, focusing on four fundamental aspects. First, a harder asphalt emulsion will be assessed, which will increase the mechanical strength of the new asphalt concrete. Second, work must be done on the optimization of the magnetic induction machine to improve this application. Thirdly, work will have to be done to assess deeply the mechanical performance, such as the feasibility of the mixtures at low temperatures or fatigue resistance. In addition, environmental and economic impact assessment will be carried out to validate the technology.

CRediT authorship contribution statement

Christopher Delafuente-Navarro: Writing – original draft, Visualization, Validation, Methodology, Investigation, Formal analysis, Data curation, Conceptualization. **Pedro Lastra-González:** Writing – review & editing, Visualization, Validation, Supervision, Methodology, Investigation, Formal analysis, Conceptualization. **Irune Indacoechea-Vega:** Writing – review & editing, Visualization, Validation, Supervision, Data curation, Conceptualization. **Daniel Castro-Fresno:** Writing – review & editing, Validation, Supervision, Resources, Project administration, Funding acquisition.

Declaration of Competing Interest

The authors declare that they have no known competing financial interests or personal relationships that could have appeared to influence the work reported in this paper.

Data availability

Data will be made available on request.

Acknowledgments

This publication is part of the project SICA+ (Ref. PDC2021-120824-I00), financed by MICIU/AEI/10.13039/501100011033 and by the European Union Next Generation EU/PRTR. The authors acknowledge and thank these institutions.

The authors would like to thank Vicente Pérez Mena and María Del Mar Colás from Cepsa Comercial Petróleo S.A. for their collaboration. At the same time, we thank Andrés Rivas Sánchez, Maria Teresa Rodriguez Valero and Paula Del Rio Gandarillas, whose excellent work in the laboratory gave a fundamental added- value to the development of this research.

References

[1] G. Sun, W. Ning, X. Jiang, K. Qiu, Z. Cao, Y. Ding, A comprehensive review on asphalt fume suppression and energy saving technologies in asphalt pavement industry, Sci. Total Environ. vol. 913 (2024) 169726, https://doi.org/10.1016/j.scitotenv.2023.169726.
[2] X. Fang, A. Garcia-hernandez, P. Lura, Overview on cold cement bitumen emulsion asphalt, RILEM Tech. Lett. vol. 1 (2016) 116–121, https://doi.org/10.21809/rilemtechlett.2016.23.
[3] S. Jain, B. Singh, Cold mix asphalt: an overview, J. Clean. Prod. vol. 280 (2021) 124378, https://doi.org/10.1016/j.jclepro.2020.124378.
[4] L.P. Thives, E. Ghisi, Asphalt mixtures emission and energy consumption: a review, Renew. Sustain. Energy Rev. vol. 72 (2017) 473–484, https://doi.org/10.1016/j.rser.2017.01.087.
[5] C. Ling, H.U. Bahia, Development of a volumetric mix design protocol for dense-graded cold mix asphalt, J. Transp. Eng., Part B: Pavements vol. 144 (4) (2018) 04018039, https://doi.org/10.1061/jpeodx.0000071.
[6] I.N.A. Thanaya, S.E. Zoorob, J.P. Forth, A laboratory study on cold-mix, cold-lay emulsion mixtures, Proc. Inst. Civ. Eng.: Transp. vol. 162 (1) (2009) 47–55, https://doi.org/10.1680/tran.2009.162.1.47.
[7] S.S. Dash, A.K. Chandrappa, U.C. Sahoo, Design and performance of cold mix asphalt – a review, Constr. Build. Mater. vol. 315 (2022), https://doi.org/10.1016/j.conbuildmat.2021.125687.
[8] K.R. Usman, M.R. Hainin, M.K.I. Mohd Satar, M.N. Mohd Warid, S.N. N. Kamarudin, S. Abdulrahman, Palm oil fuel ash application in cold mix dense-graded bituminous mixture, Constr. Build. Mater. vol. 287 (2021) 123033, https://doi.org/10.1016/j.conbuildmat.2021.123033.
[9] T.A. Tedla, D. Singh, B. Showkat, Effects of air voids on comprehensive laboratory performance of cold mix containing recycled asphalt pavement, Constr. Build. Mater. vol. 368 (2023) 130416, https://doi.org/10.1016/j.conbuildmat.2023.130416.
[10] Z. Liu, L. Sun, A review of effect of compaction methods on cold recycling asphalt mixtures, Constr. Build. Mater. vol. 401 (2023) 132758, https://doi.org/10.1016/j.conbuildmat.2023.132758.
[11] Z. Liu, L. Sun, A review of effect of compaction methods on cold recycling asphalt mixtures, Constr. Build. Mater. vol. 401 (2023) 132758, https://doi.org/10.1016/j.conbuildmat.2023.132758.
[12] P. Meena, G.R.R. Naga, P. Kumar, Effect of mechanical properties on performance of cold mix asphalt with recycled aggregates incorporating filler additives, Sustainability (Switzerland) vol. 16 (1) (2024), https://doi.org/10.3390/su16010344.
[13] A.I. Nassar, M.K. Mohammed, N. Thom, T. Parry, Characterisation of high-performance cold bitumen emulsion mixtures for surface courses, Int. J. Pavement Eng. vol. 19 (6) (2018) 509–518, https://doi.org/10.1080/10298436.2016.1176165.
[14] A. Graziani, C. Iafelice, S. Raschia, D. Perraton, A. Carter, A procedure for characterizing the curing process of cold recycled bitumen emulsion mixtures, Constr. Build. Mater. vol. 173 (2018) 754–762, https://doi.org/10.1016/j.conbuildmat.2018.04.091.
[15] Asphalt Institute, "Institute Manual Series No.19, Third edition," 1997. doi: (AI MS 19).
[16] A. Graziani, A. Grilli, C. Mignini, A. Balzi, Assessing the field curing behavior of cold recycled asphalt mixtures, Adv. Mater. Sci. Eng. vol. 2022 (2022), https://doi.org/10.1155/2022/4157090.
[17] A. Graziani, C. Godenzoni, F. Cardone, M. Bocci, Effect of curing on the physical and mechanical properties of cold-recycled bituminous mixtures, Mater. Des. vol. 95 (2016) 358–369, https://doi.org/10.1016/j.matdes.2016.01.094.
[18] S. Saboundjian, R.L. McHattie, Alaska's dense-graded high-float emulsion surface treatments: a new mix design, Transp. Res Rec. vol. 2 (1989) (2007) 161–168, https://doi.org/10.3141/1989-60.
[19] H. Al Nageim, S.F. Al-Busaltan, W. Atherton, G. Sharples, A comparative study for improving the mechanical properties of cold bituminous emulsion mixtures with cement and waste materials, Constr. Build. Mater. vol. 36 (2012) 743–748, https://doi.org/10.1016/j.conbuildmat.2012.06.032.
[20] T. Saadoon, A. Garcia, B. Gómez-Meijide, Dynamics of water evaporation in cold asphalt mixtures, Mater. Des. vol. 134 (2017) 196–206, https://doi.org/10.1016/j.matdes.2017.08.040.
[21] J. Serfass, J. Poirier, J. Henrat, and X. Carbonneau, Influence of curing on cold mix mechanical performance, 2004, pp. 365–368. doi: DOI10.1617/14130.
[22] M.-C. Liao, C.-C. Luo, T.-Y. Wang, X. Xie, Developing effective test methods for evaluating cold-mix asphalt patching materials, J. Mater. Civ. Eng. vol. 28 (10) (2016) 1–10, https://doi.org/10.1061/(asce)mt.1943-5533.0001639.
[23] Z. Liu, L. Sun, J. Zhai, W. Huang, A review of design methods for cold in-place recycling asphalt mixtures: design processes, key parameters, and evaluation, J. Clean. Prod. vol. 370 (May) (2022) 133530, https://doi.org/10.1016/j.jclepro.2022.133530.
[24] P. Deb, K. Lakshman Singh, Mix design, durability and strength enhancement of cold mix asphalt: a state-of-the-art review, Innov. Infrastruct. Solut. vol. 7 (1) (2022) 1–22, https://doi.org/10.1007/s41062-021-00600-2.
[25] W. Yang, J. Ouyang, Y. Meng, B. Han, Y. Sha, Effect of curing and compaction on volumetric and mechanical properties of cold-recycled mixture with asphalt emulsion under different cement contents, Constr. Build. Mater. vol. 297 (2021) 123699, https://doi.org/10.1016/j.conbuildmat.2021.123699.
[26] P. Lastra-González, I. Indacoechea-Vega, M.A. Calzada-Pérez, D. Castro-Fresno, A. Vega-Zamanillo, Mechanical assessment of the induction heating as a method to

accelerate the drying process of cold porous asphalt mixtures, Constr. Build. Mater. vol. 208 (2019) 646–650, https://doi.org/10.1016/j.conbuildmat.2019.03.053.
[27] I. Pérez, B. Gómez-Meijide, A.R. Pasandín, A. García, G. Airey, Enhancement of curing properties of cold in-place recycling asphalt mixtures by induction heating, Int. J. Pavement Eng. vol. 22 (3) (2021) 355–368, https://doi.org/10.1080/10298436.2019.1609674.
[28] C. DeLaFuente-Navarro, P. Lastra-González, M.Á. Calzada-Pérez, D. Castro-Fresno, Rheological and mechanical consequences of reducing the curing time of cold asphalt mixtures by means of magnetic induction, Case Stud. Constr. Mater. (2023), https://doi.org/10.1016/j.cscm.2023.e02573.
[29] T. Geckil, S. Issi, C.B. Ince, Evaluation of prina for use in asphalt modification, Case Stud. Constr. Mater. vol. 17 (2022), https://doi.org/10.1016/j.cscm.2022.e01623.
[30] F. Chen, R. Balieu, A state-of-the-art review of intrinsic and enhanced electrical properties of asphalt materials: theories, analyses and applications, Mater. Des. vol. 195 (2020) 109067, https://doi.org/10.1016/j.matdes.2020.109067.
[31] C. DeLaFuente-Navarro, P. Lastra-González, M.Á. Calzada-Pérez, D. Castro-Fresno, Rheological and mechanical consequences of reducing the curing time of cold asphalt mixtures by means of magnetic induction, Case Stud. Constr. Mater. (2023), https://doi.org/10.1016/j.cscm.2023.e02573.
[32] Á. García, E. Schlangen, M. Van De Ven, Q. Liu, A simple model to define induction heating in asphalt mastic, Constr. Build. Mater. vol. 31 (2012) 38–46, https://doi.org/10.1016/j.conbuildmat.2011.12.046.
[33] Á. García, E. Schlangen, M. van de Ven, Q. Liu, Electrical conductivity of asphalt mortar containing conductive fibers and fillers, Constr. Build. Mater. vol. 23 (10) (2009) 3175–3181, https://doi.org/10.1016/j.conbuildmat.2009.06.014.
[34] A. García, J. Norambuena-Contreras, M.N. Partl, P. Schuetz, Uniformity and mechanical properties of dense asphalt concrete with steel wool fibers, Constr. Build. Mater. vol. 43 (2013) 107–117, https://doi.org/10.1016/j.conbuildmat.2013.01.030.
[35] Q. Liu, W. Yu, S. Wu, E. Schlangen, P. Pan, A comparative study of the induction healing behaviors of hot and warm mix asphalt, Constr. Build. Mater. vol. 144 (2017) 663–670, https://doi.org/10.1016/J.CONBUILDMAT.2017.03.195.
[36] E. Jeoffroy, F. Bouville, M. Bueno, A.R. Studart, M.N. Partl, Iron-based particles for the magnetically-triggered crack healing of bituminous materials, Constr. Build. Mater. vol. 164 (2018) 775–782, https://doi.org/10.1016/j.conbuildmat.2017.12.223.
[37] J.M. Yang, J.K. Kim, D.Y. Yoo, Effects of amorphous metallic fibers on the properties of asphalt concrete, Constr. Build. Mater. vol. 128 (2016) 176–184, https://doi.org/10.1016/j.conbuildmat.2016.10.082.
[38] C. Yang, et al., Enhanced induction heating and self-healing performance of recycled asphalt mixtures by incorporating steel slag, J. Clean. Prod. vol. 366 (March) (2022), https://doi.org/10.1016/j.jclepro.2022.132999.
[39] C. Fu, F. Wang, K. Liu, Q. Liu, P. Liu, M. Oeser, Inductive asphalt pavement layers for improving electromagnetic heating performance, Int. J. Pavement Eng. vol. 24 (1) (2023), https://doi.org/10.1080/10298436.2022.2159401.
[40] Á. García, E. Schlangen, M. Van De Ven, Q. Liu, A simple model to define induction heating in asphalt mastic, Constr. Build. Mater. vol. 31 (2012) 38–46, https://doi.org/10.1016/j.conbuildmat.2011.12.046.
[41] C. Fu, K. Liu, P. Liu, M. Oeser, Experimental and numerical investigation of magnetic converge effect of magnetically conductive asphalt mixture, Constr. Build. Mater. vol. 360 (October) (2022) 129626, https://doi.org/10.1016/j.conbuildmat.2022.129626.
[42] H. Xu, et al., Research on gradient characteristics and its prediction method of induction heating asphalt concrete, Constr. Build. Mater. vol. 309 (September) (2021) 124920, https://doi.org/10.1016/j.conbuildmat.2021.124920.
[43] P. Lastra-González, M.Á. Calzada-pérez, D. Castro-fresno, Á. Vega-zamanillo, I. Indacoechea-vega, Porous asphalt mixture with alternative aggregates and crumb-rubber modified binder at reduced temperature vol. 150 (2017) 260–267, https://doi.org/10.1016/j.conbuildmat.2017.06.008.
[44] A.H.A. Alhaddad, Construction of a complex shear modulus master curve for Iraqi asphalt binder using a modified sigmoidal fitting, Int. J. Sci. Eng. Technol. Res. vol. Vol.04 (Iss, no) (2015) 0682–0690, doi: ISSN 2319-8885.
[45] A. Gupta, P. Lastra-Gonzalez, J. Rodriguez-Hernandez, M. González González, D. Castro-Fresno, Critical assessment of new polymer-modified bitumen for porous asphalt mixtures, Constr. Build. Mater. vol. 307 (May) (2021), https://doi.org/10.1016/j.conbuildmat.2021.124957.
[46] F. Moreno-Navarro, M. Sol-Sánchez, A. Jiménez del Barco, M.C. Rubio-Gámez, Analysis of the influence of binder properties on the mechanical response of bituminous mixtures, Int. J. Pavement Eng. vol. 18 (1) (2017) 73–82, https://doi.org/10.1080/10298436.2015.1057138.
[47] N. Saboo, P. Kumar, Analysis of different test methods for quantifying rutting susceptibility of asphalt binders, J. Mater. Civ. Eng. vol. 28 (7) (2016) 1–8, https://doi.org/10.1061/(asce)mt.1943-5533.0001553.
[48] M. Mirsepahi, J. Tanzadeh, S.A. Ghanoon, Laboratory evaluation of dynamic performance and viscosity improvement in modified bitumen by combining nanomaterials and polymer, Constr. Build. Mater. vol. 233 (2020) 117183, https://doi.org/10.1016/j.conbuildmat.2019.117183.
[49] M. Lagos-Varas, et al., Influence of limestone filler on the rheological properties of bituminous mastics through susceptibility master curves, Constr. Build. Mater. vol. 231 (2020), https://doi.org/10.1016/j.conbuildmat.2019.117126.
[50] M.D.I. Domingos, A.L. Faxina, Rheological behaviour of bitumens modified with PE and PPA at different MSCR creep-recovery times, Taylor & Francis (2015), https://doi.org/10.1080/10298436.2014.953503.
[51] G. Cuciniello, P. Leandri, G. Polacco, G. Airey, M. Losa, Applicability of time-temperature superposition for laboratory-aged neat and SBS-modified bitumens, Constr. Build. Mater. vol. 263 (2020) 120964, https://doi.org/10.1016/j.conbuildmat.2020.120964.
[52] Z. Zhou, X. Gu, J. Jiang, F. Ni, Y. Jiang, Nonrecoverable behavior of polymer modified and reclaimed asphalt pavement modified binder under different multiple stress creep recovery tests, Transp. Res Rec. vol. 2672 (28) (2018) 324–336, https://doi.org/10.1177/0361198118782029.
[53] AASHTO, Standard Specification for Performance-Graded Asphalt Binder. 2023. doi: 10.1520/D6373-21A.